Reactions between Guanidine and Cu^+ in the Gas Phase. An Experimental and Theoretical Study

A. Luna, B. Amekraz, J.-P. Morizur, and J. Tortajada*,†

Laboratoire de Chimie Organique Structurale, Université Pierre et Marie Curie, UMR 172, Boîte 45, 4 Place Jussieu, 75252, Paris Cedex 05, France

O. Mó and M. Yáñez*,‡

Departamento de Química, C-9. Universidad Autónoma de Madrid, Cantoblanco, 28049-Madrid, Spain

Received: March 21, 1997; In Final Form: June 12, 1997[⊗]

Mass spectrometry measurements reveal that the reactions between guanidine and Cu^+ in the gas phase leads predominantly to the loss of ammonia. The corresponding mechanisms were investigated by means of DFT calculations at the B3LYP/6-311+G(2df,2p)//B3LYP/6-311G(d,p) level. The attachment of Cu^+ takes place preferentially at the imino nitrogen, while attachment at the amino leads to a local minimum which lies almost 26 kcal/mol higher in energy. The estimated guanidine−Cu^+ binding energy is 77.9 kcal/mol. Hence, guanidine is predicted to be a stronger base than ammonia when the reference acid is Cu^+, although this basicity difference is about 11 kcal/mol smaller than that found when the reference acid is H^+. Two possible reaction channels, with almost equal activation barriers, lead to the loss of NH_3. One of them yields the $H_2N-CN-Cu^+$ complex while the other yields the $HNCNHCu^+$ complex. The structures and bonding characteristics of both products are discussed. Their estimated heats of formation are 225 ± 2 and 237 ± 2 kcal/mol, respectively. The structures and the relative stabilities of the complexes which can be formed by the solvation of these two products by ammonia have been also investigated since they are essential to explain the unimolecular NH_3-loss processes observed.

Introduction

The past two decades have witnessed a great development of the ion chemistry in the gas phase from both the theoretical and the experimental points of view, in an effort to gather reliable information on processes related to different fields as plasma chemistry, atmospheric chemistry, or interstellar chemistry.[1] A great deal of effort was also devoted to the determination of the intrinsic reactivities of molecules. In this respect, it must be mentioned that besides the intrinsic basicities of different compounds with respect to the proton,[2] there are also basicity scales with respect to other reference acids as CH_3^+ or metal monocations.[3−5] The cationization of neutral molecules by association with metal cations is actually one of the most important topics in ion chemistry in the gas phase.[6] Very often metal cation association is accompanied by significant bond activation effects, which lead to specific fragmentations.[6] On the other hand, the gas-phase metal cationization of some organic molecules is relevant from the biological point of view since it can address a deeper insight into the intrinsic (nonsolvated) interactions between metal ions and biomolecules involved in the biochemical reactions governing the cations exchange at cellular level. These kinds of reactions often involve transition metal cations. In addition, transition metal cations are not only ubiquitous in living systems but also useful in analytical mass spectrometry. In recent years, metal ion chemical ionization have proven to be a very useful tool to investigate the amino acid sequence of peptides.[7−9] Recently, Cerda *et al.*[10] determined the relative Cu^+ ion affinities of the 20 common α-amino acids and showed that arginine exhibits the highest Cu^+ affinity due to the strongly basic guanidyl side group**.** This functional group in the arginine side chain has attracted the interest of chemists as it has been recognized to afford specific features to this amino acid. Tang *et al.*[11] have shown that alkali metal ion complexes of peptides containing *C*-terminal arginine residues undergo specific fragmentation pathways. At the same time there is a lack of reliable information on these ion−molecule reactions from the theoretical point of view since most of the existing calculations were carried out at the semiempirical or low ab initio levels,[12] far below the state of the art level that is nowadays standard for most of the quantum chemistry applications. However, the size of molecules of biological interest is so large that their theoretical treatment at high ab initio levels becomes economically prohibited. A reasonably good alternative is to modelize these big molecules by smaller systems which present similar active sites within similar environments.

In this context, we have considered it of interest to study the gas-phase reactions between guanidine and Cu^+ ion in order to provide some fundamental information about this special interaction. It is worth noting that guanidine has its own relevance from the biological point of view in consideration of its interesting biochemical properties. There is not much information on the gas-phase reactivity of guanidine, and its gas-phase proton affinity was not measured until very recently.[13] That combined experimental and theoretical study showed[13] guanidine to be a base of moderate strength in the gas phase, even though it is one of the strongest bases known in solution. Guanidine presents, as an additional interesting feature, in particular when association with metal cations is concerned, three nitrogen basic centers which can lead to several kinds of complexations. A theoretical study[14] of its association with metal monocations, namely Li^+, Na^+, Mg^+, and Al^+, showed

* Corresponding authors.
† Tel: 33 (1) 44 27 31 10. Fax: 33 (1) 44 27 25 68. E-mail: jeat@moka.ccr.jussieu.fr.
‡ Tel: 34 (1) 397 49 53. Fax: 34 (1) 397 41 87. E-mail: manuel@idefix.qui.uam.es.
⊗ Abstract published in *Advance ACS Abstracts,* August 1, 1997.

S1089-5639(97)01030-X CCC: $14.00

that the global minima of the corresponding potential energy surfaces correspond to the addition of the metal cation to the imino nitrogen, although for the particular case of Li^+ and Na^+ complexes the structures where the metal cation bridges between the imino and one of the amino nitrogens are also very stable. This behavior seems to be a direct consequence of the electrostatic nature of the ion−neutral interactions in these kinds of systems. Cu^+ presents in its ground state a d^{10} closed-shell structure, with an empty 4s orbital; hence, it is reasonable to expect the reactions of guanidine and Cu^+ to follow quite different patterns. The interaction with this transition metal monocation should have important covalent contributions, as it has been found in reactions of Cu^+ with simple hydrocarbons and with other small nitrogen bases. Furthermore, from the biological perspective, the Cu^+ reactions also play an important role.[15,16]

The rationalization of the most important features of the fast atom bombardment (FAB) mass spectra of guanidine−Cu^+ requires a reliable description of the corresponding potential energy surface, in terms of the different local minima and the transient species connecting them. It is nowadays well established that G2-type calculations[17] perform very well for this purpose. Unfortunately, these kinds of calculations are very expensive for systems as large as guanidine−Cu^+ complexes. A reasonably good alternative would be the use of density functional theory (DFT) methods together with flexible enough basis sets, which have been shown[13,18,19] to provide proton affinities in close agreement with both the G2 and the experimental values. To verify that a similar performance can be expected when dealing with Cu^+ complexes, we have studied, in a previous paper,[20] the interaction of Cu^+ with sp, sp^2, and sp^3 nitrogen containing model compounds, namely NH_3, NH_2-CH_3, $NHCH_2$, and HCN. Since our system contains as a basic centers sp^2- and sp^3-hybridized nitrogens, we can reasonably assume that the accuracy of our estimations will be of the same order of magnitude as those found for these smaller systems.

Here we report an experimental and theoretical study on the unimolecular reactivity of Cu^+ ions with guanidine. This work is organized as follows: the unimolecular dissociation processes of [guanidine−Cu^+], studied by means of mass ionic kinetic energy spectroscopy (MIKES) will be first discussed, and then our interest will be focused on the analysis of the corresponding potential energy surface by means of high-level DFT calculations.

Experimental Section

The mass spectrometric measurements were recorded on a double-focusing ZAB-HSQ mass spectrometer (Fisons Instruments) of BeqQ configuration[21] (B and E represent the magnetic and electric sectors, q is a collision cell consisting of a rf-only quadrupole, and Q is a mass-selective quadrupole). This mass spectrometer is equipped with a FAB ion source using the following conditions: accelerating voltage 8 kV, neutral xenon beam of 7 keV, and neutral current of ∼10 A. Guanidine hydrochloride was dissolved in a thioglycerol matrix to which had been added a few drops of a saturated aqueous $CuCl_2$ solution. A few microliters of the resulting mixtures was transferred onto the FAB probe tip. The Cu^+ ions are likely formed from Cu^{2+} salt (e.g., $CuCl_2$) by oxidation/reduction processes as has been previously postulated.[22] Copper ions are seen in their natural abundance, i.e., 69% ^{63}Cu and 31% ^{65}Cu; the results presented here refer to the more abundant isotope (at *m/z* 63).

The unimolecular reactions of the mass-selected organometallic ions, corresponding to [guanidine−Cu^+] metastable ions, which take place in the second field-free region (2nd FFR) behind the magnet, were studied by mass-analyzed ion kinetic energy (MIKE) spectroscopy. This technique consists in focusing the relevant ion magnetically into the 2nd FFR and detecting the products of spontaneous fragmentations by scanning the electrostatic analyzer, E. The MIKE spectra were recorded at a resolving power of ∼1000.

Guanidine hydrochloride was purchased from Aldrich and used without further purification.

Computational Details

The geometries of the different species under consideration have been optimized by using the hybrid density functional B3LYP method, i.e., Becke's three-parameter nonlocal hybrid exchange potential[23] with the nonlocal correlation functional of Lee, Yang, and Parr.[24] This approach has been shown[25] to yield reliable geometries for a wide variety of systems. For some of the guanidine−Cu^+ complexes and some of the products of the reaction considered, the B3PW91 method[26] has been also used in order to check whether the inclusion of the Perdew−Wang nonlocal correlation functional instead of that of Lee, Yang, and Parr may have some influence on the optimized geometries of Cu^+-containing systems. All these calculations were performed using the all-electron basis of Watchers−Hay[27] for Cu and the 6-311G(d,p) basis set for the remaining atoms of the system. The harmonic vibrational frequencies of the different stationary points of the potential energy surface (PES) have been calculated at the same level of theory used for their optimization in order to identify the local minima and the transition states (TS), as well as to estimate the corresponding zero-point energies (ZPE). To identify what minima are connected by a given TS, we have performed intrinsic reaction coordinate (IRC) calculations at the same level of theory.[28] IRC calculations have been used also to confirm the nature of weakly bound stationary points in those cases where the imaginary frequencies were small.

As mentioned above, we have shown that association energies for Cu^+ complexes obtained at the DFT/6-311+G(2df,2p) level are in reasonably good agreement with those estimated in the framework of the G2 theory.[17] Hence, the final energies of the different species under study were obtained in DFT/6-311+G-(2df,2p) single-point calculations at the aforementioned DFT-optimized geometries. It should be noted that the basis set employed in these DFT calculations differs from that used in the G2 formalism in the number of sets of d polarization functions included. We have tested,[20] however, taking the Cu^+−NH_3 complexes as a suitable benchmark case, that the binding energies so obtained do not differ significantly from those calculated with the larger basis set, while the time of calculation is considerably reduced.

The basis set superposition error (BSSE) has not been considered in the present study since, as has been previously reported,[29] for DFT and DFT/HF hybrid methods this error is usually small, when the basis set expansion is sufficiently flexible.

In spite of the well-known lack of B3LYP in describing dissociation processes, the possible contributions in binding energies of Cu^+ configurations other than d^{10} have been discarded: as showed by Ricca et al.,[30] Cu^+ turns out to be a good case in which the asymptotic energy corrections for higher states in Cu^+ may be neglected.

To investigate the nature of the Cu−N bond and, in general, the bonding features of the complexes under consideration, we used the natural bond orbital (NBO) analysis of Weinhold et al.,[31] and the atoms in molecules (AIM) theory of Bader.[32] The

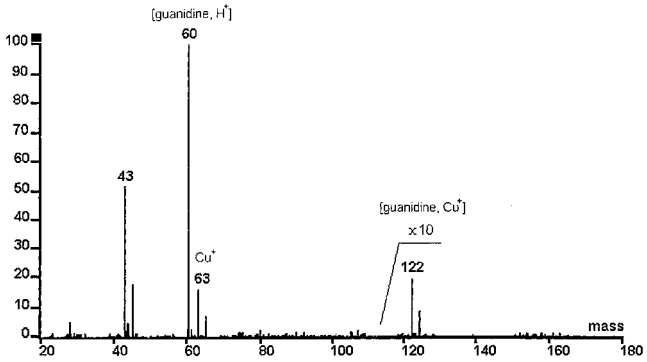

Figure 1. FAB spectrum of guanidine dissolved in a matrix of thioglycerol containing $CuCl_2$.

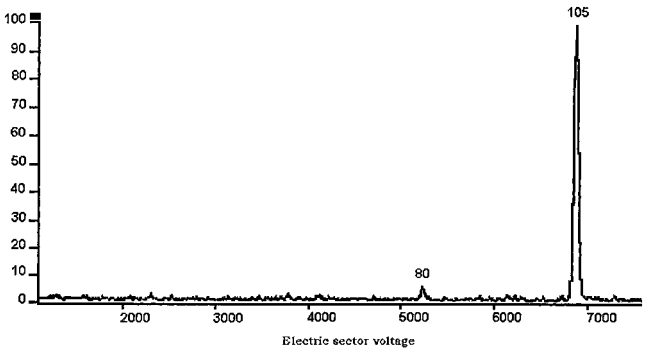

Figure 2. MIKE spectrum of the [guanidine−Cu]$^+$ complex at *m/z* 122.

first formalism allowed us to obtain the atomic natural total charges and a description of the bonding in terms of the natural hybrids centered on each atom. Using the second approach we have located the bond critical points (i.e., points where the electron density function, $\rho(\mathbf{r})$, is minimum along the bond path and maximum in the other two directions), and we have evaluated the ellipticities of the bonds, which give useful information regarding the double-bond character of the linkages. The Laplacian of the density, $\nabla^2\rho(\mathbf{r})$, as has been shown in the literature,[32] identifies regions of the space wherein the electronic charge is locally depleted ($\nabla^2\rho > 0$) or built up ($\nabla^2\rho < 0$). The former situation is typically associated with interactions between closed-shell systems (ionic bonds, hydrogen bonds, and van der Waals molecules), while the latter characterizes covalent bonds, where the electron density concentrates in the internuclear region.

All calculations have been carried out using the GAUSSIAN94 series of programs.[33] The AIM analysis was performed using the AIMPAC series of programs.[34]

Results and Discussion

Reactivity. Fast atom bombardment of guanidine dissolved in a matrix of thioglycerol containing $CuCl_2$ produces abundant [guanidine, Cu]$^+$ adduct ion at *m/z* 122. In addition, protonated guanidine at *m/z* 60 and *m/z* 43 (corresponding to [C, N_2, H_3]$^+$ ions) are also observed, as shown in the mass spectrum in Figure 1.

The unimolecular behaviour of the [guanidine, Cu]$^+$ complex was investigated. The MIKE spectrum presented in Figure 2 shows that the *m/z* 122 ion undergoes fragmentation by two distinct pathways. The major fragmentation is the elimination of NH_3 leading to the ion at *m/z* 105 (base peak of the MIKE spectrum), assigned to the [C, N_2, H_2, Cu]$^+$ complex. A very narrow but characteristic fragment at *m/z* 80 (6%) is also observed and may be assigned to the [NH_3, Cu]$^+$ complex.

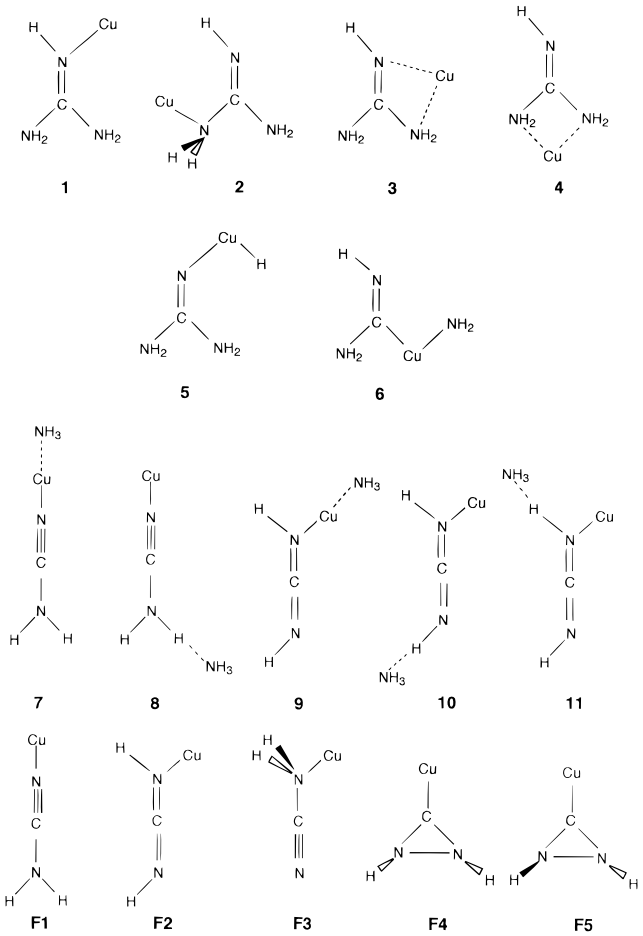

Figure 3. Schematic representation of the relevant structures to be investigated.

In order to elucidate the possible pathways leading to the observed experimental products, we propose the study of the complexes depicted in Figure 3. The first set of structures (**1**−**4**) corresponds to the possible formation of mono and bicoordinated Cu^+ adducts. In the second set (**5**−**6**) we have explored the possibility of insertion of Cu^+ in the N−H and Cu−NH_2 bonds, respectively. We discarded the possibility of insertion in the C═N bond because of its strength. The next set of structures on Figure 3 (**7**−**11**) corresponds to the structures that can lead to the possible fragmentation products (**F1**−**F5**).

[H_5, C, N_3, Cu]$^+$ Complexes. Structure and Bonding. The B3LYP optimized geometries of the different minima associated with the guanidine−Cu^+ PES are given in Figure 4, where the B3PW91 optimized geometries were not included for the sake of conciseness, although they are available from the authors upon request. In this respect, it must be mentioned that no significant differences have been found between B3LYP and B3PW91 optimized structures. Taking the values of the rotational constants as suitable and sensitive indexes of the geometry similarities, the averaged deviation from B3PW91 to B3LYP values was 1.2%, the maximum deviation being 3.7%.

The total energies of these species as well as their relative stabilities are summarized in Table 1. The most stable guanidine−Cu^+ complex **1** corresponds to the adduct of Cu^+ at the imino nitrogen. The association of Cu^+ to the amino nitrogen leads to a much less stable complex, **2** (about 26 kcal/mol less stable). This is consistent with the expected higher basicity of the imino nitrogen of guanidine. In fact, at similar levels of accuracy protonation at the amino nitrogen of guanidine was predicted to be 33.7 kcal/mol less favorable than protonation at the imino group. It should also be noted that complexes **2**

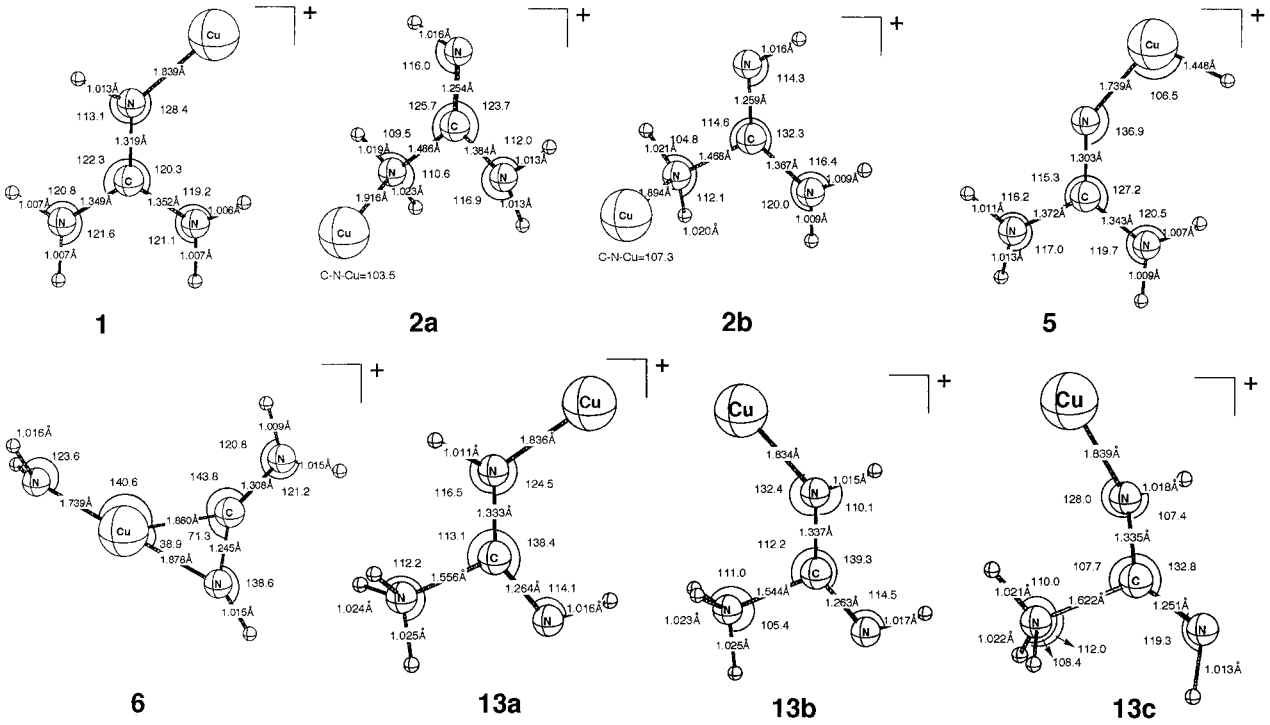

Figure 4. B3LYP/6-311G(d,p) optimized geometries for some relevant minima of the $[H_5, N_3, C, Cu]^+$ potential energy surfaces. Bond distances are in Å, angles in deg.

TABLE 1: Total Energies, ZPE (hartrees), and Relative Energies (kcal/mol) of the Stationary Points Correspondig to the Hypersurface $[H_5, N_3, C, Cu]^+$ at the B3LYP/ 6-311+G(2df,2p)//B3LYP 6-311G(d,p) + ZPE Level

system	absolute E	ZPE	E_{rel} (E_{rel} + ZPE)
1	−1845.760 354	0.077 202	0.0 (0.0)
	−1845.637 360[a]	0.077 568[a]	0.0(0.0)[a]
2a	−1845.713 927	0.078 368	29.1 (29.9)
	−1845.590 886[a]	0.078 724[a]	29.2 (30.0)[a]
2b	−1845.719 907	0.078 290	25.4 (26.0)
5	−1845.636 171	0.071 144	77.9 (74.4)
	−1845.512 265[a]	0.071 522[a]	78.5 (74.7)[a]
6	−1845.678 893	0.073 862	51.1 (49.0)
7	−1845.797 594	0.074 869	−23.4 (−24.9)
8	−1845.657 587[b]	0.072 735	11.9 (9.1)[b]
9	−1845.778 877	0.074 960	−11.6(−13.0)
10	−1845.640 008[b]	0.072 057	22.9(19.7)[b]
13a	−1845.703 006	0.077 520	36.0(36.2)
13b	−1845.700 092	0.078 149	37.8(38.4)
13c	−1845.606 353[b]	0.076 774	44.0(43.8)[b]
TS1	−1845.672 714	0.072 198	55.0 (51.7)
TS2a	−1845.674 935	0.073 147	53.6(51.1)
TS2b	−1845.673 047	0.073 313	54.8(52.3)
TS3	−1845.650 940	0.072 621	68.7(65.9)
TS4a	−1845.690 023	0.073 397	44.1(41.7)
TS4b	−1845.683 245	0.073 140	48.4(45.9)
guanidine	−205.458 260	0.075 980	
	−205.377 147[a]	0.076 298[a]	
Cu^+	−1640.176 694		
	−1640.136 711[a]		
guanidine + Cu^+	−1845.634 954	0.075 980	78.7 (77.9)
	−1845.513 858[a]	0.076 298[a]	77.5 (76.8)[a]

[a] B3PW91 values with the same basis set. [b] Values considered at B3LYP/6-311G(d,p).

present two alternative conformations separated ca. 4 kcal/mol. The most stable conformer **2b** corresponds to the association with the amino group *trans* with respect to the imino hydrogen.

It is worth mentioning that no chelated structures with the metal cation bridging between the imino and one of the amino nitrogens have been found (structures **3** and **4** in Figure 3). Actually all attempts to optimize the structure **3** led, without activation barrier, to the global minimum **1**. Similarly, structure **4** where the metal cation bridges between both amino nitrogens was found to be unstable as it collapses to the local minimum **2b**.

TABLE 2: Bonding Characteristics of Complexes 1 and 2b[a]

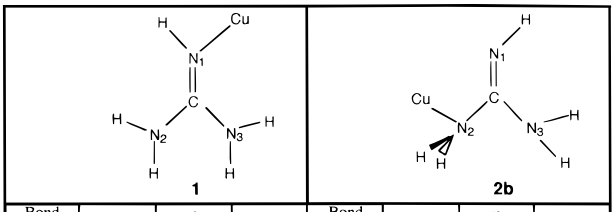

Bond	ρ	$\nabla^2\rho$	ε	Bond	ρ	$\nabla^2\rho$	ε
Cu-N_1	0.126	0.544	0.045	Cu-N2	0.113	0.488	0.017
C-N_1	0.358	-1.136	0.221	C-N_1	0.405	-1.205	0.308
C-N_2	0.331	-1.022	0.164	C-N2	0.261	-0.706	0.062
C-N_3	0.331	-1.037	0.167	C-N_3	0.320	-0.969	0.162

[a] The charge densities are in e·au^{-3} and the Laplacian, $\nabla^2\rho$, in e·au^{-5}. ϵ is the ellipticity.

It is important to emphasize that the aforementioned chelated structures were found[14] to be stable in guanidine−Li^+ and guanidine−Na^+ complexes, where the ion−neutral interactions are essentially electrostatic. This seems to indicate that guanidine−Cu^+ interactions have a different nature. Actually, both the NBO and the AIM analyses indicate that N−Cu linkage in guanidine complexes have an important covalent character. As illustrated in Table 2, the charge densities at the Cu−N bcps of both complexes **1** and **2b** are almost 1 order of magnitude larger than the typical values found in ionic linkages. It can be also observed that the charge density in complex **1**, where Cu^+ is associated with the imino nitrogen is almost equal[20] to that found in complexes between $H_2C{=}NH$ and Cu^+. Similarly, the charge density at the N−Cu bond in complex **2b** is almost equal to that reported[20] for complexes involving NH_3 and CH_3NH_2 molecules. This seems to indicate that values of ρ_c around 0.13 e·au^{-3} are typical of N(sp^2)−Cu^+ linkages and those of 0.11 e·au^{-3} are characteristic of N(sp^3)−Cu^+ bonds. The NBO description of the N−Cu^+ linkages in complexes **1** and **2b** is

TABLE 3: Harmonic Vibrational Frequencies (cm^{-1}) and Assignments for Neutral Guanidine and Complex 1

freq	assign	freq	assign
3654	NH_2 a str	3723	NH_2 a str
3648	NH_2 a str	3717	NH_2 a str
3550	NH_2 s str	3611	NH_2 s str i.p.
3545	NH_2 s str	3600	NH_2 s str o.p.
3494	NH str	3572	NH str
1745	CN str	1686	CNH_2 str + NH_2 sciss
1645	NH_2 sciss o.p.	1677	CNH_2 str + NH_2 sciss
1631	NH_2 sciss i.p.	1635	CNH str + NH_2 sciss
1450	NCN assym str + HNC bend	1556	CN str + NH_2 sciss
1196	NH_2 rock	1329	CNH bend
1139	HNC bend	1127	NH_2 rock
1100	NCN a str + NH_2 rock	1064	NH_2 rock
938	NCN s str	1021	CN str
814	NH pyram + NH_2 pyram	729	NH−C−NH_2 bend
775	C pyram	655	C pyram
660	NH_2 wag o.p.	645	NH_2 pyram + NH pyram
580	NH_2 wag i.p.	524	NH_2 twist
542	NCN rock	515	NCH rock
477	NCN sciss	364	Cu−N str
406	NH_2 twist	350	NH_2 wag + C−NH_2 twist
360	NH_2 twist	316	NH_2 wag
		241	NH_2 wag
		131	C−N−Cu bend
		101	C−N−Cu bend

consistent with the AIM picture. It shows the existence of a bonding MO involving one of the N-hybrids and a sd hybrid of Cu^+, as proposed before by Marinelli et al.[35] and has been seen in our previous study.[20] The dominant contribution of the N-hybrid and the strong s character of the sd hybrid of Cu^+ permit to classify this interaction as a dative bond, which involves the lone pair of the base and the initially empty 4s orbital of the metal cation. Hence Cu^+ constitutes an intermediate situation between H^+, which yields strongly covalent linkages and Li^+, which yields almost purely ionic bonds. In agreement with this, when the reference acid is Cu^+, the enhanced basicity of guanidine with respect to ammonia is 22 kcal/mol, which is about 6 kcal/mol greater and 11 kcal/mol smaller than the estimated enhancements when the reference acids are Li^+ and H^+, respectively. Also the vibrational frequency shifts upon Cu^+ association (see Table 3) are analogous but smaller than those found upon protonation. In complex **1** all the NH_2 stretches appear systematically shifted to higher frequencies with respect to those of the neutral. The N−H stretch appears also blue-shifted, while the C−NH stretch is red-shifted. The influence on the NH_2 twisting and wagging modes is also significantly large. The former appears blue-shifted and the latter red-shifted. As a consequence, while in the neutral the twisting mode appears at lower frequencies than the wagging, in the complex it is the other way around. The N−Cu stretching frequency is predicted to be observed at 364 cm^{-1}.

We have also considered the possibility of insertion of the metal cation into the N−H bond of the imino group or into the C−NH_2 linkages. The first process leads to the local minimum **5**, which is predicted to be 74.4 kcal/mol less stable than the global minimum. The second insertion mechanism leads to a cyclic species **6** (see Figure 4), where the Cu−NH_2 moiety metal appears to be interacting with the π cloud of C═N bond. Nevertheless, this form also lies high in energy (ca. 49.0 kcal/mol) with respect to the global minimum. These results are consistent with the fact that, in general, Cu^+ yields addition−elimination reactions rather than insertion reactions. Hence, we may safely conclude that species **5** and **6** will not play a significant role in the gas-phase reactions between guanidine and Cu^+.

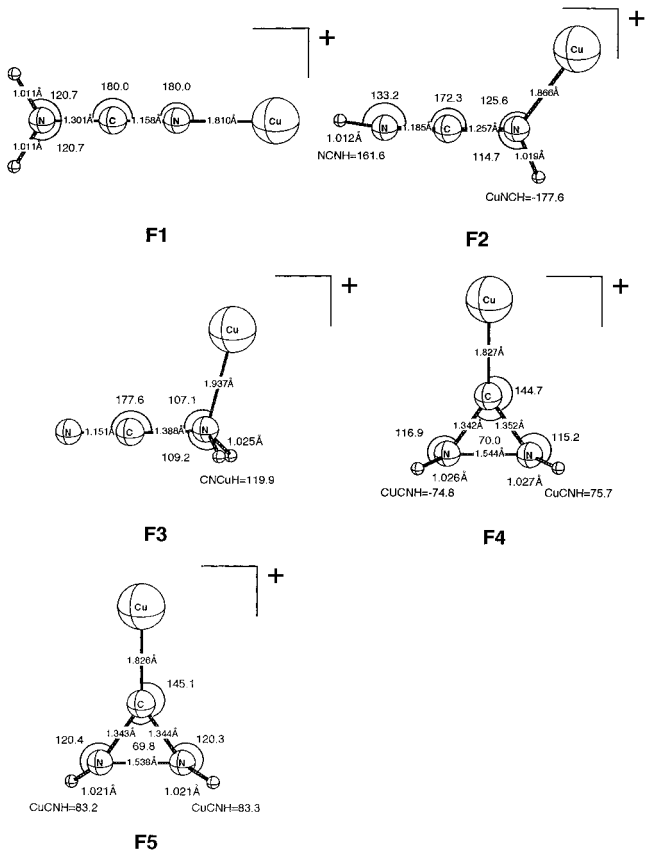

Figure 5. B3LYP/6-311G(d,p) optimized geometries for the relevant stationary points of the $[H_2, N_2, C, Cu]^+$ potential energy surfaces. Bond distances are in Å, angles in deg. Species **F1** and **F2** are the likely products of the guanidine−Cu^+ reactions.

TABLE 4: Total Energies, ZPE (hartrees), and Relative Energies (kcal/mol) of the Stationary Points Corresponding to the Hypersurface $[H_2, N_2, C, Cu]^+$ at the B3LYP/6-311+G(2df,2p)//B3LYP/6-311G(d,p) + ZPE Level[a]

system	absolute *E*	ZPE	E_{rel} (E_{rel} + ZPE)
F1	−1789.123 657	0.035 228	0.0 (0.0)
	−1789.017 939	0.035 393	0.0 (0.0)
F2	−1789.104 658	0.035 150	11.9 (11.8)
	−1788.999 384	0.035 283	11.6 (11.6)
F3	−1789.069 900	0.037 306	33.7 (35.0)
	−1788.963 795	0.037 401	34.0 (35.3)
F4	−1788.904 160[b]	0.033 426	90.0 (88.8)[b]
	−1788.805 879[b]	0.033 752	87.9 (86.8)[b]
F5	−1788.913 131[b]	0.034 347	84.4 (83.8)[b]
	−1788.815 086[b]	0.034 718	82.1 (81.7)[b]
NH_3	−56.586 387	0.034 299	
	−56.563 819	0.034 463	

[a] The second entry corresponds to B3PW91 method using the same basis set. [b] Values considered at B3LYP/6-311G(d,p).

NH_3 Loss Reaction Products. In order to characterize unambiguously the products of this reaction, we have systematically explored the $[H_2, C, N_2, Cu]^+$ PES. Off the 12 possible conformers that can be considered, the five structures (**F1**−**5**) schematized in Figure 5 were found to be local minima. The corresponding total energies as well as their relative stabilities are given in Table 4. These values show that the most stable cation **F1** corresponds to the adduct of Cu^+ to the cyano nitrogen of the H_2N−C≡N molecule, while the association to one of the nitrogen atoms of the HN═C═NH species to yield **F2** is predicted to be 11 kcal/mol less favorable. At this point it is worth mentioning that this energy difference does not reflect a similar energy gap between the corresponding neutrals, which are almost degenerate. Actually, the HN═C═NH isomer is

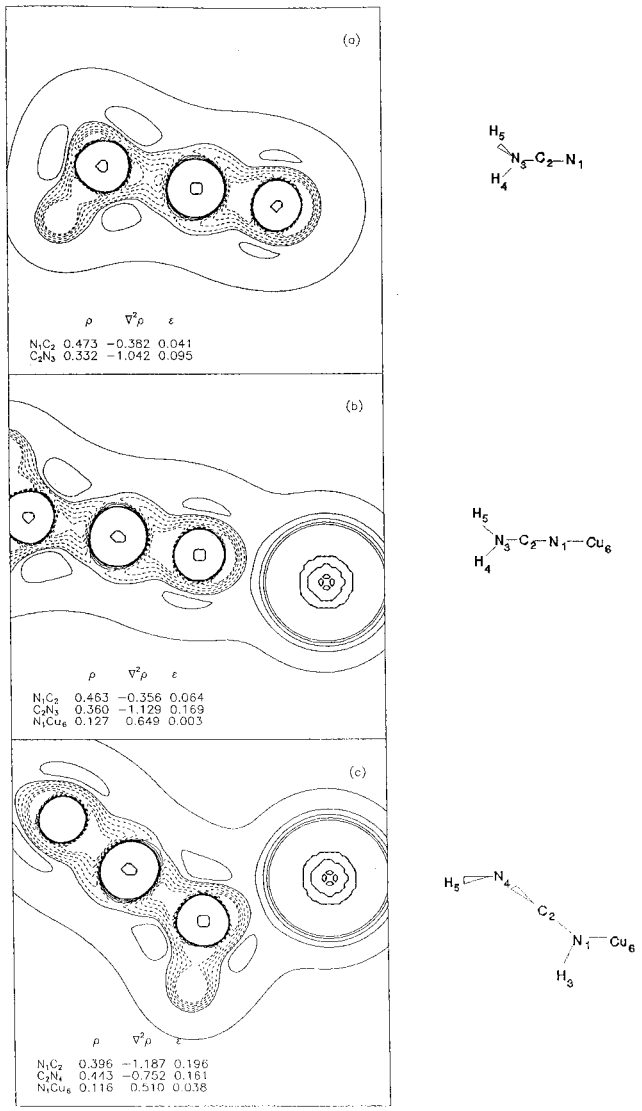

Figure 6. Contour maps of the Laplacian of the charge density of species (a) neutral H_2N-CN, (b) complex **F1**, (c) complex **F2**. Positive values of $\nabla^2\rho$ are denoted by solid lines and negative values by dashed lines. Contour values in au are ±0.05, ±0.25, ±0.50, ±0.75, and ±0.95. The charge density ρ, in e·au^{-3}, its Laplacian $\nabla^2\rho$, in e·au^{-5}, and the ellipticity values at the corresponding bond critical points are given.

TABLE 5: Harmonic Vibrational Frequencies (cm^{-1}) and Assignments for Neutral NH_2CN and Complex F1

freq	assign	freq	assign
3642	NH_2 a str	3661	NH_2 a str
3551	NH_2 s str	3554	NH_2 s str
2362	**N−C**≡N str	2416	**N−C**≡N str
1636	NH_2 bend	1615	NH_2 bend
1198	NH_2 rock	1233	C−NH_2 str
1097	C−NH_2 str	1136	NH_2 rock
571	NH_2 wag + NCN bend	534	NCN bend o.p.
491	NCN bend o.p.	440	NCN bend i.p.
416	NCN bend i.p.	384	Cu−N str
		244	NH2 wag
		145	CuNC bend i.p.
		103	CuNC bend o.p.

predicted to be only 0.2 kcal/mol more stable than the $H_2N-C\equiv N$ isomer at the B3LYP/6-311G** level. When the basis set is enlarged, the relative stability of HNCNH slightly increases, and the energy gap with respect to $H_2N-C\equiv N$ becomes 1.5 kcal/mol. Hence, we must conclude that $H_2N-C\equiv N$ is a much stronger base with respect to Cu^+ than its HN=C=NH isomer. In fact, the metal cation dissociation energy of complex

TABLE 6: Harmonic Vibrational Frequencies (cm^{-1}) and Assignments for Neutral HNCNH and Complex F2[a]

freq	assign	freq	assign
3590	NH str i.ph.	3629	NH_b str
3588	NH str o.ph.	3507	NH_a str
2238	NCN a str	2289	NCN a str
1287	NCN s str	1316	C−NCu str
919	HNC bend	1232	H_a NC bend
918	HNC bend	723	H_a NC + H_bNC bend
729	CN twist	657	CNH_b + NCN bend
540	NCN bend	631	NCN bend + Cu−N str
537	NCN bend	526	NCH_b + NCN bend
		424	Cu−N str
		356	CN twist
		140	CNCu bend

[a] H_a refers to H attached at N−Cu and H_b to the other one.

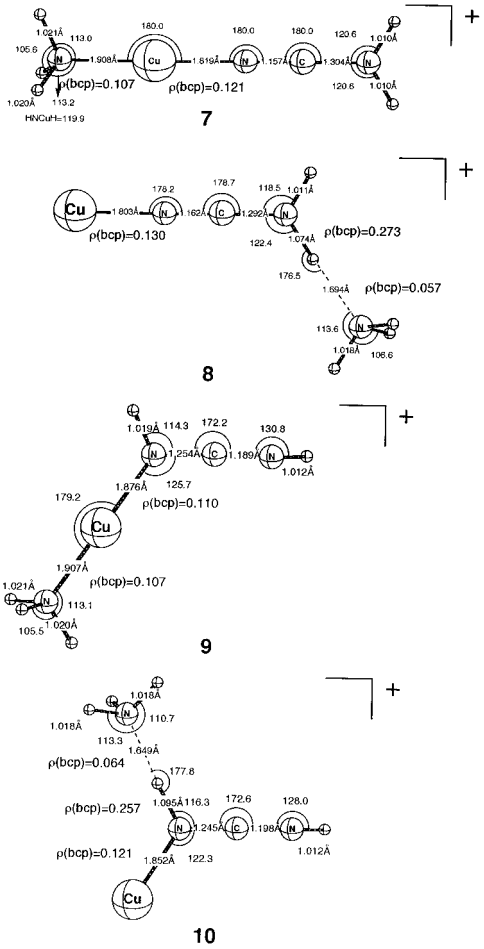

Figure 7. B3LYP/6-311G(d,p) optimized geometries for the complexes that can be formed by solvation of species **F1** and **F2** by ammonia. The charge density (ρ) in e·au^{-3} at the bond critical point for some selected bonds is also included.

F1 (64 kcal/mol) is 14 kcal/mol greater than that predicted for the complex between the unsubstituted, HCN, parent compound.[20] The enhanced basicity of $H_2N-C\equiv N$ species reflects the donor ability of the amino substituent. In fact, while in the neutral $H_2N-C\equiv N$ species the amino group is not planar, it becomes strictly planar in complex **F1** to favor the conjugation of the H_2N lone pair with the C≡N π-system. This is clearly reflected in the corresponding charge distributions and their Laplacians (see Figure 6a,b). The polarization of charge toward the metal cation implies a charge depletion at the C≡N bond, which becomes longer. Simultaneously, the charge density increases at the C−NH_2 bond, which becomes shorter. Also the ellipticity of the latter increases due to a sizable increase of

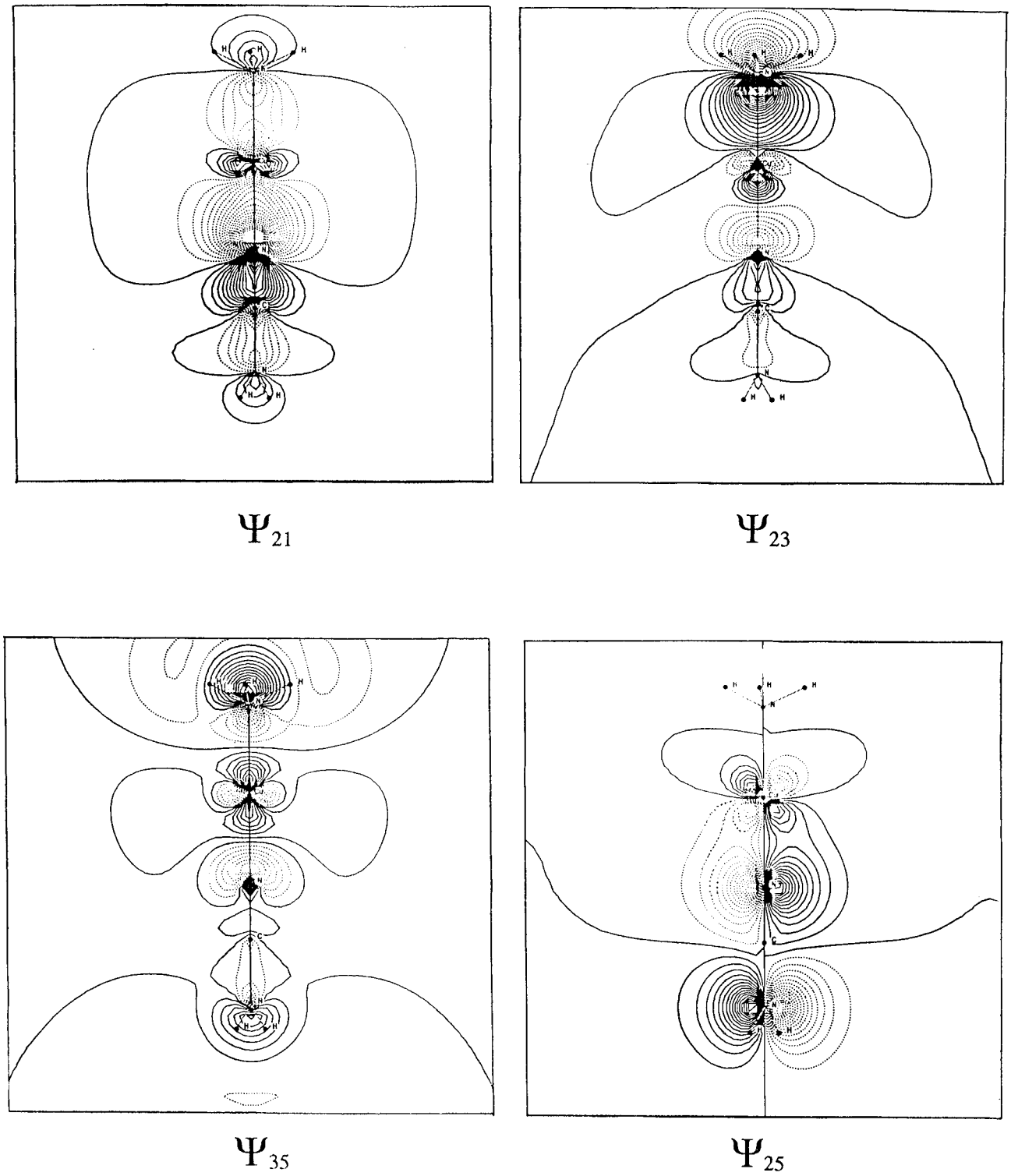

Figure 8. Canonical molecular orbitals for species **7** involved in the N−Cu−N bondings.

its double bond character. This charge density redistribution is consistent with the shift undergone by the corresponding harmonic vibrational frequencies. As can be seen from the values in Table 5, the C−NH_2 stretch is significantly shifted to higher frequencies. As for guanidine, the NH_2 stretching modes are blue-shifted, while the NH_2 wagging is red-shifted. The N−Cu stretch is found at 384 cm^{-1}.

It is also worth noting that HNCNH is much less basic than H_2CNH.[20] This is an expected result if one takes into account that we have replaced a H_2C group by a much more electronegative HNC group. Consistently, the charge density at the N−Cu^+ bcp in complex **F2** (see Figure 6c) is lower than expected for a N(sp^2)−Cu^+ bond. It can be also observed that the C−N bond to which the metal cation is attached becomes longer. Accordingly, its bcp charge density decreases. As far as the vibrational frequencies are concerned (see Table 6) it can be observed that while in the neutral the NCN stretching modes appear as symmetric and asymmetric combinations, in complex **F2** they appear almost completely uncoupled. It is worth noting that Cu^+ association has a dramatic effect on the torsion which appears red-shifted by 370 cm^{-1}.

Species **F3**, which corresponds to the association of Cu^+ to the amino nitrogen of the H_2N−C≡N, is about 35 kcal/mol less stable than the global minima **F1** and 24 kcal/mol less stable

than **F2**. It can be noted that this energy gap is quite similar to that reported above between the attachment of Cu^+ to the imino and the amino nitrogens of guanidine. The attachment of Cu^+ to the carbon atom of the HN═C═NH isomer yields two cyclic structures, namely **F4** and **F5**. The former has a C_s symmetry, while the latter belongs to the C_2 point group. Both lie very high in energy with respect to complex **F1**. In the light of the previous discussion we may conclude that the $[Cu, C, N_2, H_2]^+$ species produced in Cu^+ + guanidine reactions must correspond to structures **F1** and **F2**, while the formation of complex **F3** must be considered noncompetitive with respect to **F1** and **F2** production. According to our results the three reactions are clearly exothermic:

$$Cu^+ + \text{guanidine} \rightarrow \mathbf{F1} + NH_3 \qquad \Delta H_0{}^0 = -51.1 \text{ kcal/mol} \quad (1)$$

$$\rightarrow \mathbf{F2} + NH_3 \qquad \Delta H_0{}^0 = -39.3 \text{ kcal/mol} \quad (2)$$

$$\rightarrow \mathbf{F3} + NH_3 \qquad \Delta H_0{}^0 = -16.1 \text{ kcal/mol} \quad (3)$$

Reactions 1−3 may be used to estimate their heats of formation by combining the estimated reaction enthalpies with the experimental heats of formation of guanidine, ammonia and Cu^+ taken from ref 36. The values so obtained are 225 ± 2 kcal/mol for complex **F1**, 237 ± 2 kcal/mol for **F2**, and 260 ± 2 kcal/mol for complex **F3**.

Intermediates for Dissociation Products. In the Figure 3 we can see the possible complexes (**7**−**11**) which can arise from the interaction of ammonia with the $[Cu, C, N_2, H_2]^+$ species. It is important to study these kind of systems because they may arise (as we shall discuss in the following section) from unimolecular rearrangements of the adducts created initially in the primary cationization reaction, and they can be used to explain both the loss of ammonia and the minor peak at *m/z* 80. The stable structures found (see Figure 7) can be classified in two well-defined groups: (a) weakly bound species, which correspond to hydrogen-bonded complexes in which ammonia interacts with one of the hydrogen atoms of the $[Cu, C, N_2, H_2]^+$ cation (structures **8** and **10**) and (b) tightly bound systems in which ammonia interacts with the Cu^+ (structures **7** and **9**). Among the latter, the most stable complex is **7**, which corresponds to the addition of the NH_3 molecule to cation **F1**. The important point is that this structure is extremely stable, being 25 kcal/mol more stable than the Cu^+ adduct to the imino nitrogen of guanidine (**1**). This clearly indicates the existence of a quite strong interaction between the ammonia molecule and the metal ion, which according to the bcp charge densities (see Figure7), leads to a bond Cu−NH_3 which is only slightly weaker than the linkage between the metal ion and the H_2N−C≡N moiety. This is not surprising since it has been already reported[37] that in the gas phase, Cu^+ prefers to be dicoordinated. Theoretical calculations[38] have shown previously that sdσ hybridization reduces the repulsion of ligand−metal on both sides of Cu^+ at the same time, and therefore the linear situation of N−Cu−N is specially favorable because two ligands can share the energetic cost of this hybridization. This is consistent with (a) the fact that chelated structures **3** and **4** do not exist since the geometrical constraints restrict the interactions N−Cu−N avoiding the energetic stabilization produced by the sdσ hybridization, and (b) the characteristics of the canonical MO's directly involved in the metal cation bonding. The interaction of the sdσ hybrid of the Cu with the sp(N) and

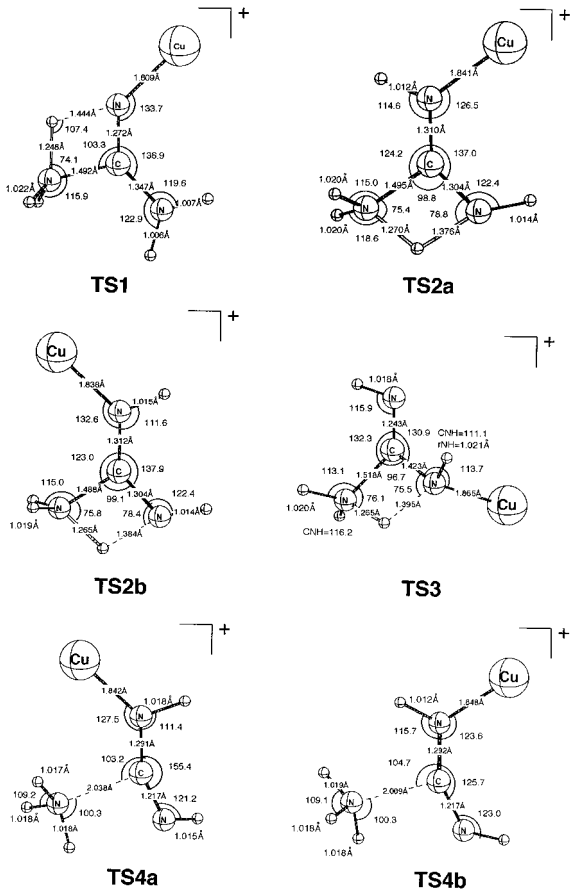

Figure 9. B3LYP/6-311G(d,p) optimized geometries for relevant transition states of the $[H_5, N_3, C, Cu]^+$ potential energy surfaces. Bond distances are in Å, angles in deg.

sp^3(N) hybrids of the NC−NH_2 and NH_3 moieties leads to three MO's, namely Ψ_{21}, Ψ_{23}, and Ψ_{35} (see Figure 8). The first two are doubly occupied while the latter is empty. As expected, Ψ_{21} is N−Cu−N bonding, Ψ_{23} is H_3N−Cu bonding and Cu−$NCNH_2$ antibonding, and Ψ_{35} is N−Cu−N antibonding. Also interesting, the existence of Ψ_{25} MO (see Figure 8) illustrates the π back donation capacity of Cu, through an interaction between one of its d orbital of the appropriate symmetry and a π orbital of the NC−NH_2 moiety.

Consistent with the previous arguments, the NBO population of Cu^+ at complex **F1** is $4s^{0.35}3d^{9.73}$, while in Cu^+-dicoordinated complex **7** is $4s^{0.59}3d^{9.63}$, which shows the significant change in the population of s orbital of Cu^+. In the case of complex **8** the population analysis for Cu^+ is very similar ($4s^{0.38}3d^{9.72}$) to that in **F1**, as could be expected from the monocoordination of Cu^+ in both structures. It is also worth noting that the linkages between Cu and ammonia in both complexes, **7** and **9** are rather similar in the sense that they exhibit about the same bcp charge density and the same bond length (see Figure 7). Consistently, the energy gap between both complexes is practically equal to that found between the unsolvated species **F1** and **F2**.

Reaction Profiles for the Fragmentation Processes. Since the experimental findings discussed in the previous section show mainly spontaneous decomposition with loss of NH_3, we paid special attention to elucidate the possible mechanisms which could lead to this loss. Figure 9 shows the geometries of the transition states involved in the evolution of the possible adducts.

Assuming that the first step of the reaction Cu^+−guanidine generates the more stable adduct **1** (see Figure 10), one possible mechanism would correspond to a hydrogen transfer from the

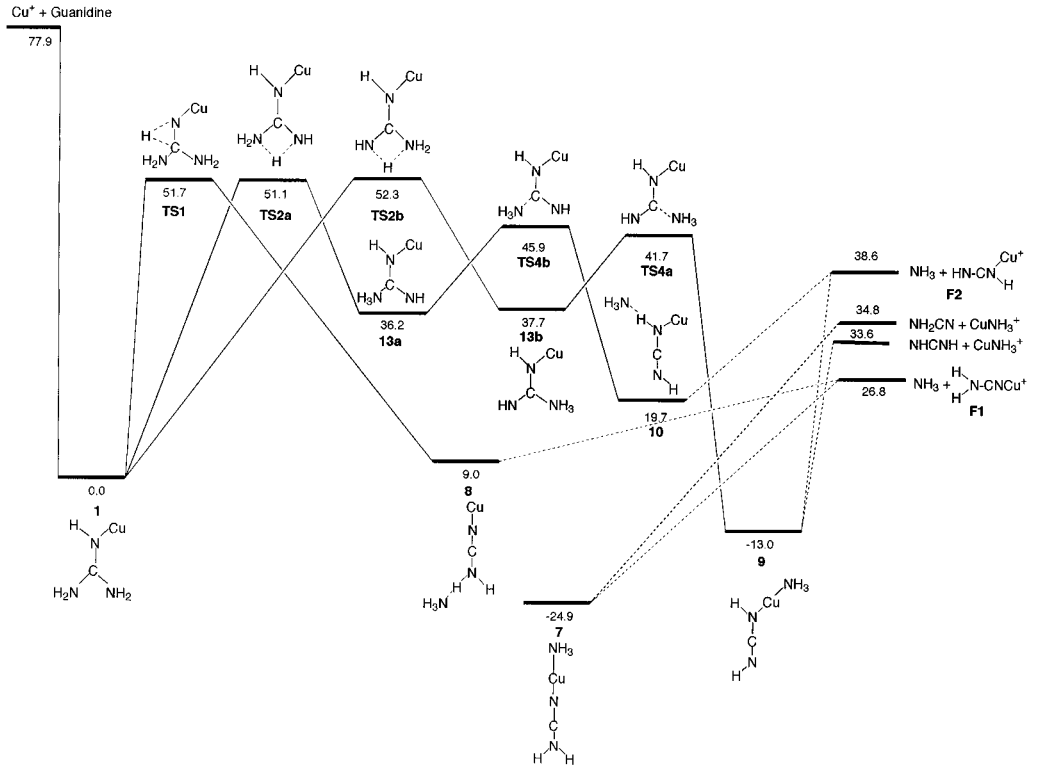

Figure 10. Energy profile for the PES associated with the guanidine−Cu^+ reactions starting at complex **1**. Relative energies are in kcal/mol.

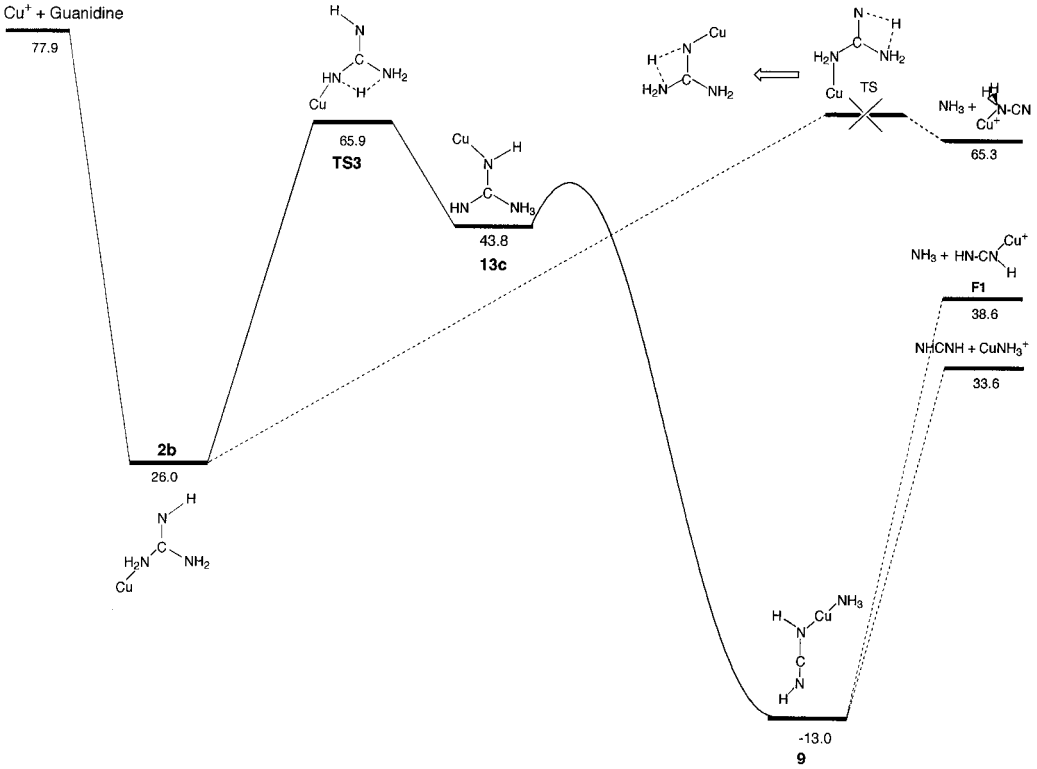

Figure 11. Energy profile for the PES associated with the guanidine−Cu^+ reactions starting at complex **2b**. Relative energies are in kcal/mol.

imino nitrogen to one of the amino nitrogens, which takes place through the transient species **TS1**. The connectivity of this transient structure was established by means of IRC calculations. In this way it was found that **TS1** leads, in one of the directions of the reaction coordinate vector associated with the sole imaginary frequency, to the global minimum **1**, while in the opposite direction it leads to the stable complex **8**. We can assume that the loss of NH_3 is produced from **8** without barrier, to generate the products NH_3 + **F1**.

In order to confirm this assumption the H···NH_3 distance was scanned from its value in the equilibrium conformation of **8** to sufficiently long distances (7.0 Å). Those calculations confirm that no barrier exists for such a dissociation. On the other hand, all attempts to connect structures **7** and **8** failed since the increasing of the H···NH_3 distance did not lead to a reorientation of the $NH_2-C-N-Cu^+$ moiety. An alternative mechanism would involve the hydrogen transfer processes between the two amino groups of the global minimum, through the transient

species **TS2a** or **TS2b**, which lead to conformers **13a** and **13b**, respectively. A scanning of the C−NH_3 bond distance showed that structure **13a** evolves via the **TS4b** to yield the weakly bound complex **10**, which eventually dissociates to NH_3 + **F2** (see Figure 10). Similarly, the **13b** complex evolves via the homologous **TS4a** to generate the very stable dicoordinated Cu^+ complex **9**, which can dissociate to the products **F1** + NH_3, as well as to the minoritary observed products $Cu{-}NH_3^+$ + NHCNH. Figure 10 clearly shows that **F1** should be expected to be the major product of the reaction, because although the barriers involved in the formation of **F1** and **F2** are rather similar, the formation of the former is more exothermic.

Further possibilities are open if some amount of adduct **2b**, where Cu^+ is attached to the amino group of guanidine, is produced in the primary reaction. The corresponding potential energy surface has been plotted in Figure 11. One mechanism which might eventually lead to a NH_3 loss would correspond to a hydrogen transfer from the imino group of complex **2b** to the closest amino group. However, all the efforts to locate a transition state for this hydrogen transfer process failed, because all the initial geometries considered evolved to yield the **TS1** transient species. We can then conclude that such a reactive channel corresponding to the dissociation of the stable complex **2b** to yield NH_3 is not open. However, we still have the possibility of a hydrogen transfer between both amino groups through the saddle point **TS3**. The corresponding IRC calculations revealed that the hydrogen transfer leads to conformer **13c**. As in the former cases, and due to the similarity of **13b** and **13c**, we can assume that a similar barrier would connect the minima **13c** with species **9**. Here it is worth mentioning that this channel should not be favored since the formation of **2b** is 26 kcal/mol less exothermic than the formation of **1**.

It should be noticed that, in all the possibilities explored for the NH_3 loss, the initial barriers are higher in energy than the final dissociation products, but lie below the reactants (Cu^+ + guanidine) so that all the mechanisms proposed are thermodynamically accesible.

Conclusions

The reaction between guanidine and Cu^+ in the gas phase leads predominantly to the loss of ammonia. A survey of the $[H_5, N_3, C, Cu]^+$ PES carried out at the B3LYP/6-311+G(2df,-2p)//B3LYP/6-311G(d,p) level shows that the main primary product formed corresponds to the attachement of the metal cation to the imino group, while the attachment to the amino nitrogen is less favorable by 26 kcal/mol. Insertion of the metal cation into the bonds of the base leads to local minima which lie much higher in energy. These results indicate that guanidine is a stronger base than ammonia with respect to Cu^+. However, the estimated enhancement of its basicity is smaller than that found upon protonation, although higher than that calculated, at similar levels of accuracy, when the reference acid is Li^+. An analysis of the electron density of the global minimum shows that a dative bond from the nitrogen lone pair to the initially empty 4s orbital of Cu^+ is responsible for the N−Cu linkage. The corresponding charge redistribution of the neutral is reflected in significant shifts of the harmonic vibrational frequencies.

Several reactive channels, with almost equal activation barriers, lead to the loss of ammonia. Thermodynamically speaking, a greater rate in the formation of **F1** is expected, as is observed experimentally. We have deeply examined the processes leading to the generation, and the complexes **7**−**10** (which could be considered as ammonia-solvated **F1** and **F2** complexes) are essential to describe the loss of NH_3. The solvation of these products by ammonia molecules takes place preferentially at the metal, which indicates that Cu^+ is able to accept charge from the lone pairs of two bases simultaneously, since the second basis contributes to the energetic cost of the hybridization sdσ of Cu^+ used to form the bonds.

Acknowledgment. This work was partially supported by the DGICYT Project No. PB93-0289-C02-01 and by the Action Integrée Franco-Espagnole Picasso 96093. A.L. acknowledges specially the CEE for a grant.

References and Notes

(1) See for instance: Armentrout, P. B.; Baer, T. *J. Phys. Chem.* **1996**, *100*, 12866, and references therein.

(2) Taft, R. W.; Tompson, R. D. *Prog. Phys. Org. Chem.* **1987**, *16*, 1. (b) *Gas Phase Ion Chemistry*; Bowers, M. T., Ed.; Academic Press: New York, 1979; Vol. 1 and 2; 1984, Vol. 3. (c) *Fourier Transform Mass Spectrometry, Evolution, Innovation and Application*; Buchanan, M. V., Ed.; ACS Symposium Series 359; American Chemical Society: Washington, DC, 1987.

(3) Gal, J.-F.; Taft, R. W.; McIver, R. T. Jr. *Spectrosc. Int. J.* **1984**, *3*, 96.

(4) Operti, L.; Tews, E. C.; Freiser, B. S. *J. Am. Chem. Soc.* **1988**, *110*, 3847.

(5) Taft, R. W.; Anvia, F.; Gal, J.-F.; Walsh, S.; Capon, M.; Holmes, M. C.; Hosn, K.; Oloumi, G.; Vasanwala, R.; Yazdani, S. *Pure Appl. Chem.* **1990**, *62*, 17.

(6) *Organometallic Ion Chemistry*; Freiser B. S., Ed.; Kluwer Academic Publishers, Dordrecht, 1995.

(7) McLafferty, F. W.; Schuddenmage, H. D. R. *J. Am. Chem. Soc.* **1969**, *91*, 1866.

(8) Senko, M. W.; Speir, J. P.; McLafferty, F. W. *Anal. Chem.* **1994**, *66*, 2801.

(9) Cooks, R. G. *Collision Spectroscopy*; Plenum Press: New York, 1978.

(10) Cerda, B. A.; Wesdemiotis, C. *J. Am. Chem. Soc.* **1995**, *117*, 1734.

(11) Tang, X.-J.; Thibault, P.; Boyd, R. K. *Org. Mass. Spectrom.* **1993**, *28*, 1047.

(12) Gronert, S.; Ohair, R. A. J. *J. Am. Chem. Soc.* **1995**, *117*, 2071.

(13) Amekraz, B.; Tortajada, J.; Morizur, J.-P.; González, A. I.; Mó, O.; Yáñez, M.; Leito, I.; Maria, P.-C.; Gal, J.-F. *New J. Chem.* **1996**, *20*, 1011.

(14) Leon, E.; Amekraz, B.; Tortajada, J.; Morizur, J.-P.; González, A. I.; Mó, O.; Yáñez, *J. Phys. Chem.*, in press.

(15) Lei, Q. P.; Amster, I. J. *J. Am. Soc. Mass Spectrom.* **1996**, *7*, 722.

(16) Wen, D.; Yalcin, T.; Harrison, A. G. *Rapid Commun. Mass Spectrom.* **1995**, *9*, 1155.

(17) Curtiss, L. A.; Raghavachari, K.; Trucks, G. W.; Pople, J. A. *J. Chem. Phys.* **1991**, *94*, 7221.

(18) Smith, B. J.; Radom, L. *J. Am. Chem. Soc.* **1995**, *115*, 4885.

(19) González, A. I.; Mó, O.; Yáñez, M.; León, E.; Tortajada, J.; Morizur, J.-P.; Leito, I.; Maria, P.-C.; Gal, F. *J. Phys. Chem.* **1996**, *100*, 10490.

(20) Luna, A.; Amekraz, B.; Tortajada, J. *Chem. Phys. Lett.*, **1997**, *266*, 31.

(21) Harrison, A. G.; Mercer, R. S.; Reinee, E. J.; Young, A. B.; Boyd, R. K.; March, R. E.; Porter, C. J. *Int. J. Mass Spectrom. Ion Process.* **1986**, *74*, 13.

(22) Dean, I. K. L; Bush, K. L. *Org. Mass. Spectrom.* **1988**, *24*, 733.

(23) (a) Becke, A. D. *J. Chem. Phys.* **1993**, *98*, 5648. (b) Becke, A. D. *J. Chem. Phys.* **1992**, *96*, 2155.

(24) Lee, C.; Yang, W.; Parr, R. G. *Phys Rev.* **1988**, *B37*, 785.

(25) Llamas-Saiz, A. L.; Foces-Foces, C.; Mó, O.; Yáñez, M.; Elguero, E.; Elguero, J. *J. Comput. Chem.* **1995**, *16*, 263.

(26) Perdew, J. P.; Wang, Y. *Phys. Rev.* **1992**, *B45*, 13244.

(27) (a) Watchers, A. J. H. *J. Chem. Phys.* **1970**, *52*, 1033. (b) Hay, P. J. *J. Chem. Phys.* **1977**, *66*, 4377.

(28) González, C.; Schlegel, H. B. *J. Phys. Chem.* **1989**, *90*, 2154.

(29) (a) Hertwig, R. H.; Koch, W.; Schröder, D.; Schwarz, H.; Hrusák, J.; Schwerdtfeger, P. *J. Phys. Chem.* **1996**, *100*, 12253. (b) Amekraz, B.; Tortajada, J.; Morizur, J.-P.; González, A. I.; Mó, O.; Yáñez *J. Mol. Struct. (THEOCHEM)*, in press.

(30) Ricca, A.; Bauschlicher, C. W. *Chem. Phys. Lett.* **1995**, *245*, 150.

(31) Weinhold, F.; Carpenter, J. E. *The structure of small molecules and ions*; Plenum: New York, 1988; p 227.

(32) Bader, R. F. W. *Atoms in Molecules. A Quantum Theory*; Oxford University Press: Oxford, U.K., 1990.

(33) *Gaussian 94*; Frisch, M. J.; Trucks, G. W.; Schlegel, H. B.; Gill, P:M. W.; Johnson, B. J.; Robb, M. A.; Cheeseman, J. R.; Keith, T. A.; Peterson, G. A.; Montgomery, J. A.; Raghavachari, K.; Al-Laham, M. A.; Zakrzewski, V. G.; Ortiz, J. V.; Foresman, J. B.; Cioslowski, J.; Stefanow, B. B.; Nanayaklara, A.; Challacombe, M.; Peng, C. Y.; Ayala, P. Y.; Chen, W.; Wong, M. W.; Andres, J. L.; Replogle, E. S.; Gomperts, R.; Martin, R. L.; Fox, D. J.; Binkley, J. S.; Defrees, D. J.; Baker, J.; Stewart, J. P.; Head-Gordon, M.; Gonzalez, C.; Pople, J. A. Gaussian, Inc.: Pittsburgh, PA, 1995.

(34) The AIMPAC programs package was provided by J. Cheeseman and R. F. W. Bader.

(35) Marinelli, P. J.; Squires, R. R. *J. Am. Chem. Soc.* **1989**, *111*, 4101.

(36) Lias, S. G.; Bartmess, J. E.; Liebman, J. F.; Holmes, J. L.; Levine, R. D.; Mallard, W. J. *J. Phys. Chem. Ref. Data* **1988**, *17*, Suppl. 1.

(37) Freiser, B. E. *J. Mass. Spectrom.* **1996**, *31*, 703. (b) Magnera, T. F.; David, D. E.; Stulik, D.; Orth, R. G.; Jonkman, H. T.; Michl, J. *J. Am. Chem. Soc.* **1989**, *111*, 5036.

(38) (a) Rosi, M.; Bauschlicher, C. W. *J. Chem. Phys.* **1989**, *90*, 7264. (b) Rosi, M.; Bauschlicher, C. W. *J. Chem. Phys.* **1990**, *92*, 1876. (c) Partridge, H.; Bauschlicher, C. W. *J. Phys. Chem.* **1994**, *98*, 2301. (d) Bauschlicher, C. W.; Langhoff, S. R.; Partridge, H. *J. Chem. Phys.* **1991**, *94*, 2068.